

00

Analysis of temperature-frequency dependences of dielectric permittivity and specific conductivity of vanillin

© A.S. Volkov¹, S.S. Khviyuzov²

¹ Lomonosov Northern (Arctic) Federal University,
Arkhangelsk, Russia

² N. Laverov Federal Center for Integrated Arctic Research of the Ural Branch of Russian Academy of Sciences,
Arkhangelsk, Russia AS

e-mail: khviyuzov.s@yandex.ru

Received March 29, 2024

Revised August 30, 2024

Accepted January 09, 2025

Vanillin has a wide application. It is a large-tonnage product obtained from plant biomass. The frequency-temperature dependences of the specific electrical conductivity and the components of the complex dielectric constant of vanillin were obtained by dielectric spectroscopy in the frequency range of $6.28 \cdot 10^{-2}$ – $6.28 \cdot 10^7$ rad/s and temperatures 153–433 K. The dependencies were analyzed using the Debye, Gavrilyak–Negami and Cole–Cole models. Significant changes in the electrophysical properties of vanillin during melting were shown. The presence of relaxation processes in the low, medium and high frequencies region was established. Their activation energies were determined. A comparative analysis of the characteristics of relaxers for a number of model compounds of the lignin structural units was presented in this paper. A comparative analysis of the characteristics of relaxators for vanillin, vanillin alcohol and guaiacol as model compounds of the lignin was carried out. The presence of an electron acceptor carbonyl group coupled with a benzene ring in the vanillin molecule leads to an increase in the activation energy and relaxation time of the π -electrons.

Keywords: vanillin, dielectric permittivity, relaxators, activation energy.

DOI: 10.61011/EOS.2025.02.61018.6199-24

1. Introduction

The study of the electrophysical properties of polyaromatic compounds and materials based on them is of considerable interest. The synthesis of polyaromatic compounds with various donor-acceptor substituents is an important area of these studies [1]. Aromatic compounds can be obtained in this case from lignin contained in plants in the amount of 18–35% [2].

Technical lignins are burned to generate electricity by the most common sulfate method for the production of cellulose. At the same time, lignins are a potential source of a wide range of chemical compounds owing to their multifunctional aromatic nature, therefore, the search for new ways to use the polymer and products based on it is an important area of complex processing of plant feedstock [2]. One of the areas of lignin processing is the production of low molecular weight compounds, among which vanillin has the highest demand [3,4]. Vanillin is commonly used in the food and pharmaceutical industries, it is applied in organic synthesis for the production of polymers, including polymers with low dielectric properties for the microelectronic industry [5–7]. The study of the conductive and dielectric properties of vanillin is an relevant task for this reason.

The vanillin molecule contains phenolic hydroxyl, methoxyl, and carbonyl groups conjugated to a benzene

ring. The phenolic hydroxyl group is the main reaction center in the molecule. The presence of a conjugated electron acceptor carbonyl group significantly increases the protolytic (pK_a 7.4) and reduces the redox properties of the reaction center (effective oxidation potential 897 mV) compared with guaiacol (10.0 un. and 770 mV) [8]. Vanillin belongs to dielectrics according to the value of specific electrical conductivity. The activation or „hopping“ is the main mechanism of charge movement in a molecule. We assessed the effect of the functional nature on electrophysical properties based on the analysis of the frequency-temperature dependences of the complex dielectric constant, using the identification of individual types of relaxers and the assessment of their main characteristics (frequency or relaxation time and activation energy). Relaxers are understood as charges or systems of charges that make „hops“ when excited [9, 10]. The purpose of this study is to determine the characteristics of relaxers in the vanillin molecule by dielectric spectroscopy over a wide range of alternating electric field frequencies and temperatures corresponding to different phase states. The study of the electrophysical properties of vanillin and their comparison with other model compounds of lignin will make it possible to predict changes of the properties of the natural polymer in the most common oxidative processes.

2. Materials and methods

Vanillin (3-methoxy-4-hydroxybenzaldehyde) produced by Merck (Germany) with a content of more than 99%, density of 1.056 g/cm³, melting point 80°C, boiling point 205°C, vapor pressure 0.0029 GPa at 25°C, molecule dipole moment of 3.78 D [11,12]. Vanillin was dried at 25°C (residual pressure 10 mm Hg.) for 24 h over silica gel in a vacuum dryer before the measurement (Mius, Russia).

The electrophysical characteristics were determined using a broadband dielectric spectrometer BDS Novocontrol Concept 80 (Germany) in the frequency range from $6.28 \cdot 10^{-2}$ to $6.28 \cdot 10^7$ rad/s and temperatures 153–433 K with an interval of 20 K, and 10 K near the melting point. Novocontrol Quatro cryosystem with liquid nitrogen vapor was used for thermal regulation. The electrical properties are determined by the electrical conductivity σ (S/m), and the dielectric properties are characterized by the real ϵ' and imaginary ϵ'' parts of the complex permittivity ϵ^* according to the Kramers–Kronig ratio [13]:

$$\epsilon^*(\omega) = \epsilon' - j\epsilon'' \quad (1)$$

The real part ϵ' describes the polarization processes in a substance, and the imaginary part ϵ'' determines the dielectric losses associated with the electrical conductivity of a substance.

Specific electrical conductivity (its real part) was calculated taking into account the geometric parameters of the measuring cell:

$$\sigma = \frac{GS}{d}, \quad (2)$$

where G is the electrical conductivity of the sample (S), S is the area (m²), d is the thickness (m).

3. Results and discussions

Differences in dipole moments cause polarization dispersion in alternating electric fields. The use of a wide frequency range of an alternating electric field makes it possible to evaluate the effect caused by the dipole, atomic, and electron polarization [14]. Measurements over a wide temperature range make it possible to determine the activation energy of the main carriers in various phase states. The frequency-temperature dependences σ , ϵ' and ϵ'' are shown in Fig. 1.

The dependence is satisfactorily described by an equation of the form $\sigma(\omega) = \sigma_0 \omega^\beta$ at temperatures below the melting point, it is described in accordance with the Debye model for specific electrical conductivity at temperatures above the melting point [15]. The nature of the dependence indicates a hopping mechanism of conduction. The applicability of various models indicates the dependence of the „hopping“ time on the state of aggregation of matter.

The component of ϵ' is practically independent of frequency at $T < 273$ K. A weak dispersion region is observed near $\omega = 1$ rad/s, and the difference between low-frequency

Table 1. Dependence parameters $\sigma(\omega) = \sigma_0 \omega^\beta$

T, K	$\sigma_0, \text{cm/m}$	β
153	$2.60 \cdot 10^{-14}$	1
173	$6.62 \cdot 10^{-14}$	0.977
193	$3.39 \cdot 10^{-14}$	0.845
213	$1.09 \cdot 10^{-13}$	0.962
233	$4.65 \cdot 10^{-13}$	0.837
253	$3.00 \cdot 10^{-13}$	0.879
273	$3.90 \cdot 10^{-13}$	0.861
293	$9.69 \cdot 10^{-13}$	0.856
313	$5.18 \cdot 10^{-13}$	0.852

and high-frequency values is about 0.2. The low-frequency component of the dielectric constant increases to values of 6–8 in the temperature range below the melting point, 273–353 K. The value of the high-frequency component increases by 1 after melting, several relaxation processes appear, and new polarization mechanisms are activated. The values of $\epsilon' = 1$ at $T < 313$ K indicate the presence of an electronic type of polarization and the exclusively dielectric properties of the material at these temperatures.

The imaginary part ϵ'' is represented taking into account the through-conduction [16]:

$$\epsilon'' = \epsilon''_{\text{exp}} - \frac{\sigma_S}{\sigma_0 \omega}, \quad (3)$$

where ϵ''_{exp} are the experimental values of the imaginary part of the complex permittivity, σ_S is the low-frequency component of the specific electrical conductivity, ϵ_0 is the electrical constant, $8.85 \cdot 10^{-12}$ F/m.

The extremum corresponds to relaxation processes on dependencies $\epsilon''(\omega)$. For instance, a low-frequency extreme is observed for temperatures below the melting point, and medium- and high-frequency extremes are observed for a sample in the liquid state. This makes it possible, using the Debye frequency dispersion model, to determine the time of relaxation processes from the frequency of the extremum and estimate the activation energy. Frequency dependencies allow making slices at fixed frequencies and constructing temperature dependencies. Fig. 2 shows a temperature-frequency cross-section of the values σ , ϵ' and ϵ'' .

The sharp increase of the values of ϵ' with an extremum near 350 K is attributable to a change of the structure of matter due to the phase transition to the liquid state. A sharp increase of the values of ϵ'' and σ is observed at temperatures close to melting, and an extremum is observed at low frequencies. The above temperature dependencies have several common features. Firstly, an extremum is observed near the temperature corresponding to the melting point in all dependences associated with a change in the phase state and structure of vanillin, which affects its electrophysical properties. Secondly, the increase of the electrophysical characteristics of vanillin because of pre-melting in the low and medium frequencies is more

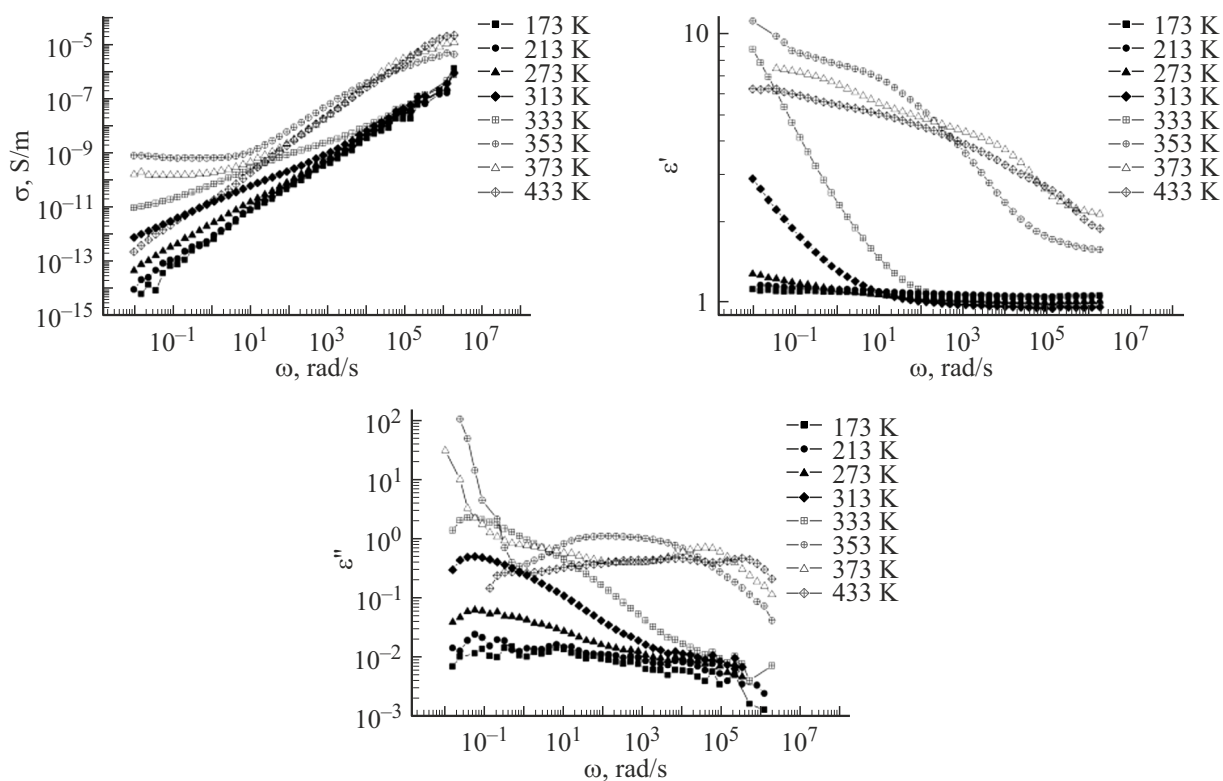


Figure 1. Frequency dependences of σ , ϵ' and ϵ'' at different temperatures.

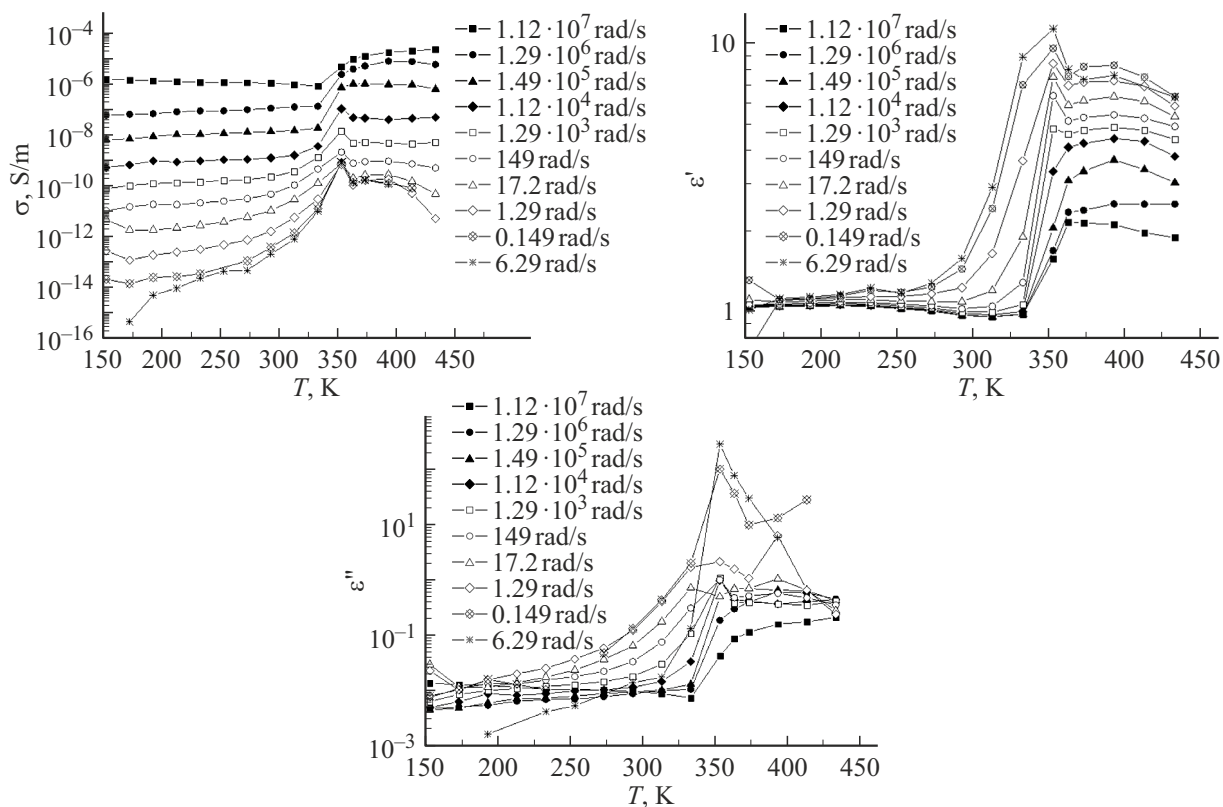


Figure 2. Temperature dependences of σ , ϵ' and ϵ'' at different frequencies.

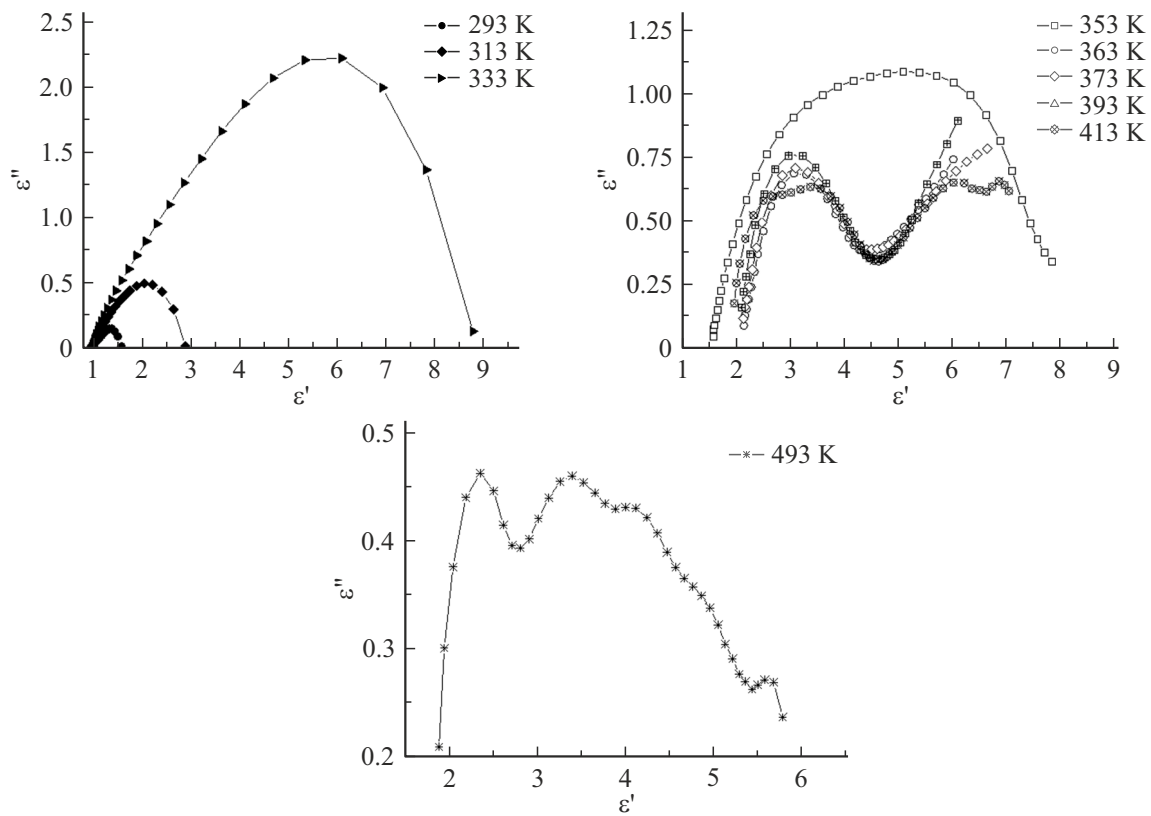


Figure 3. Cole-Cole diagrams at various temperatures.

Table 2. The results of the analysis of dependence $\sigma(\omega)$ according to the Debye frequency dispersion model

T, K	$\sigma_S, S/m$	$\sigma_\infty, S/m$	τ, s
353	$9.30 \cdot 10^{-11}$	$7.70 \cdot 10^{-6}$	$1.13 \cdot 10^{-4}$
373	$1.50 \cdot 10^{-10}$	$9.60 \cdot 10^{-6}$	$1.08 \cdot 10^{-4}$
393	$1.77 \cdot 10^{-10}$	$1.63 \cdot 10^{-5}$	$1.00 \cdot 10^{-4}$
413	$4.60 \cdot 10^{-11}$	$1.75 \cdot 10^{-5}$	$8.90 \cdot 10^{-5}$

pronounced than at high frequencies. This effect is probably attributable to the impact of the grid of H-bonds, which changes in case of the phase transition. Phenolic hydroxyl, methoxyl and carbonyl groups participate in the formation of H-bonds in the vanillin molecule which are polarized in the region of low and medium frequencies of the electric field.

The frequency dependence of specific electrical conductivity at temperatures 153–233 K (Fig. 1) is satisfactorily described by functions of the form $\sigma(\omega) = \sigma_0 \omega^\beta$, which indicates a hopping mechanism of conduction [17]. The parameters of the function at different temperatures are listed in Table 1. The exponent values β range from 0.8 to 1. The values σ_0 have the meaning of static (low frequency) electrical conductivity. The data obtained made it possible to estimate the activation energy of static conductivity

in a given temperature range according to the Arrhenius equation, which was 0.075 ± 0.005 eV:

$$\sigma = \sigma_0 \cdot \exp\left(\frac{\Delta E_a}{kt}\right). \quad (4)$$

In the temperature range corresponding to the liquid state, the dependence $\sigma(\omega)$ can be satisfactorily described by the quasi-Debye model of frequency dispersion [17]:

$$\sigma = \sigma_\infty - \frac{\sigma_\infty - \sigma_S}{1 + \omega^2 \tau^2}, \quad (5)$$

where σ_S and σ_∞ — specific electrical conductivity in the low and high frequency range, τ — relaxation time.

The values of static and high-frequency electrical conductivity were determined by limiting the transition of the dependence $\sigma(\omega)$ at $\omega \rightarrow 0$ and $\omega \rightarrow \infty$. The relaxation time was determined using the OriginPro software using the „fitting“ function and custom configuration of the approximating functions. The results of calculations and analysis are listed in Table 2.

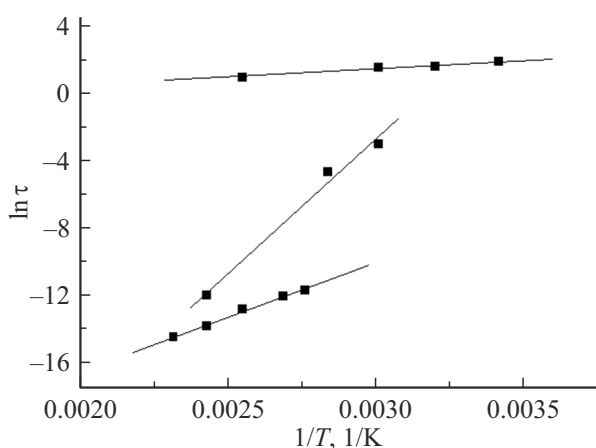
The activation energy of the relaxation time was calculated using the Arrhenius equation and amounted to 0.05 eV

$$\tau = \tau_0 \cdot \exp\left(\frac{\Delta E_a}{kT}\right). \quad (6)$$

The Debye frequency of the extremum ω_{\max} on the dependence $\varepsilon''(\omega)$ (Fig. 4) corresponds to the inverse of

Table 3. Relaxation times for the sample in the liquid state

T, K	τ , s		
	Low	medium	high
353			$1.24 \cdot 10^{-5}$
363			$8.20 \cdot 10^{-6}$
373	1.11	0.086	$3.76 \cdot 10^{-6}$
393	3.23	0.071	$1.89 \cdot 10^{-6}$
413	0.72	0.052	$7.41 \cdot 10^{-7}$
433		0.037	$4.31 \cdot 10^{-7}$

**Figure 4.** Dependence $\ln \tau (1/T)$.

the relaxation time $\tau_{\epsilon''} = 1/\omega_{\max}$ according to the frequency dispersion model. A sample in the solid state is characterized by the presence of one relaxation extremum in the low frequency region, the relaxation time of which does not depend on temperature and takes values from 1 to 10 s. At temperatures above the melting point, three extremums can be distinguished, corresponding to relaxation processes — in the low, medium, and high frequency regions. The corresponding relaxation times are listed in Table 3.

In accordance with the Arrhenius equation, the activation energy of the relaxation time of the low-frequency process was 0.90 eV, the activation energy of medium-frequency process was 0.19 eV and the activation energy of high-frequency process was 0.55 eV.

Several dispersion regions corresponding to relaxation processes are observed on dependencies $\epsilon'(\omega)$. The relaxation processes can be described by one of the frequency dispersion models combined with the dependencies $\epsilon''(\omega)$ and the satisfiability of the ratio (1). The most universal model is the Gavril'yak–Negami ratio [18]:

$$\epsilon^* = \epsilon_{\infty} + \frac{\epsilon_S - \epsilon_{\infty}}{(r + (i\omega\tau_{HN})^{\alpha})^{\beta}}, \quad (7)$$

where ϵ_S and ϵ_{∞} are the low-frequency and high-frequency permittivity of the dispersion region under study, τ_{HN} is the most probable relaxation time, α and β are parameters of the relaxation time distribution in the range of $0 < \alpha < 1$,

$0 < \beta \leq 1$. The equation becomes the Cole–Cole equation for $\beta = 1$ [19], the Davidson–Cole equation for $\alpha = 1$ [20], and the Debye equation for $\beta = 1$ and $\alpha = 1$ [21].

Separating the real ϵ' and imaginary ϵ'' parts of the complex dielectric constant

$$\epsilon' = \epsilon_{\infty} + (\epsilon_S - \epsilon_{\infty}) \cdot r^{-\frac{\beta}{2}} \cdot \cos(\beta\theta), \quad (8)$$

$$\epsilon'' = (\epsilon_S - \epsilon_{\infty}) \cdot r^{-\frac{\beta}{2}} \cdot \sin(\beta\theta), \quad (9)$$

$$r = \left(1 + (\omega\tau)^{\alpha} \cdot \sin\left(\frac{\alpha\pi}{2}\right)\right)^2 + \left((\omega\tau)^{\alpha} \cdot \cos\left(\frac{\alpha\pi}{2}\right)\right)^2, \quad (10)$$

$$\theta = \arctg\left(\frac{(\omega\tau)^{\alpha} \cdot \cos\left(\frac{\alpha\pi}{2}\right)}{1 + (\omega\tau)^{\alpha} \cdot \sin\left(\frac{\alpha\pi}{2}\right)}\right). \quad (11)$$

Various approaches are used to determine the parameters, including the computer analysis method [22–24]. The dispersion parameters obtained by any method proposed above are selected, which give the maximum convergence of the experimental and calculated curves. The dispersion regions and relaxation processes are determined by using the Cole–Cole diagrammatic technique – the dependence $\epsilon''(\epsilon')$ [20] shown in Fig.3 for various temperature ranges. One to three extremes corresponding to relaxation processes are observed on the graphs $\epsilon''(\epsilon')$ depending on the temperature. The calculated parameters are listed in Table 4.

The coefficient β is 1 for most relaxation processes, which means that the Cole–Cole dispersion relation is fulfilled. High-frequency relaxation processes attributable to π -electrons of aromatic rings were determined using the example of a wide range of lignins; medium-frequency relaxation processes attributable to hydroxyl (aliphatic and aromatic) groups, as well as chemically bound water; low-frequency relaxation processes attributable to methoxyl and carbonyl groups [20–22]. Three groups of relaxation processes can be distinguished among the data listed in Table 4 that are characterized by the dependence $\ln \tau (1/T)$ shown in Fig. 4.

The effect of the functional nature on the electrophysical properties of lignin was evaluated by comparing the results for compounds modeling its structural units (Table 5). Low-frequency relaxation processes are characterized by the lowest values of activation energies for all the studied compounds [25–30]. The highest values of ΔE_a are observed for vanillin in the mid-frequency range, which is attributable to a phase transition near the melting point and a change in the network of intra- and intermolecular H-bonds of phenolic hydroxyl groups. The highest values of ΔE_a of high-frequency process are characteristic of vanillin among the model lignin compounds, which is attributable to the redistribution of the electron density in the benzene ring due to (–)M- and (–)I-effects of the electron acceptor carbonyl group. The presence of 3.7% of carbonyl groups in the lignin sample results in an increased value of ΔE_a of high-frequency relaxation.

Table 4. Parameters of the Gavril'yak–Negami model

T, K	τ, s	α	β	ε_s	ε_∞
293	6.4	0.254	0.512	1.61	1
313	4.81	0.25	0.61	2.95	1
333	3.7	0.11	0.69	8.81	2.23
333	$5.00 \cdot 10^{-2}$	0.35	1	2.83	1
353	$1.65 \cdot 10^{-4}$	0.46	1	6.05	1.54
353	$9.50 \cdot 10^{-3}$	0.29	0.46	7.7	3.03
363	$8.30 \cdot 10^{-6}$	0.22	1	4.15	2.23
373	$5.87 \cdot 10^{-6}$	0.25	1	4.27	2.18
393	$2.83 \cdot 10^{-6}$	0.25	1	4.32	2.07
393	2.54	0.64	1	15.2	4.37
413	$1.01 \cdot 10^{-6}$	0.17	1	3.4	1.89
413	$6.50 \cdot 10^{-6}$	0.48	1	4.78	1.92
413	$7.10 \cdot 10^{-2}$	0.5	1	7.62	4.57
433	$5.40 \cdot 10^{-7}$	0.12	1	2.92	1.81
433	$2.54 \cdot 10^{-5}$	0.56	1	4.66	2.15
433	$4.00 \cdot 10^{-2}$	0.13	0.13	5.41	2.59

Table 5. Activation energy values at different frequencies

Compound	$\Delta E_a, eV$		
	Low	medium	high
Vanillin	0.12	1.30	0.55
Guaiacol (2-methoxyphenol) [29]	0.22	0.68	0.24
Vanillin alcohol (3-methoxy-4-Hydroxybenzyl alcohol) [28]	0.11	0.40	0.22
Coniferous dioxanlignin [27]	0.36	0.41	0.63

The lignin macromolecules are oxidized by oxygen in an alkaline medium to form carbonyl groups in the process of sulfate delignification which is the main industrial method for producing cellulose. Thus, a change of the functional nature of lignin as a result of the oxidation of aliphatic hydroxyl groups leads to characteristic changes of the dielectric properties of the polymer, an increase of the activation energy and high-frequency relaxation time of π -electrons of the benzene ring.

4. Conclusions

The frequency-temperature dependences of the specific electrical conductivity and complex dielectric constant of vanillin in the frequency ranges of $6.28 \cdot 10^{-2}$ – $6.28 \cdot 10^7$ rad/s and temperatures of 153–433 K have been obtained by dielectric spectroscopy. Pronounced frequency dependences of σ , ε' and ε'' near the melting point have been established. The presence of three relaxation processes in the region of low, medium and high frequencies was revealed, and their activation energies were determined. It is shown that the activation energy of the high-frequency relaxation process caused by π -electrons of the benzene ring in the vanillin molecule is

2.5 times higher than for model lignin compounds without a conjugated electron acceptor carbonyl group. Thus, oxidation processes and related differences in functional nature lead to significant changes of the dielectric properties of aromatic compounds.

Acknowledgments

The authors express their gratitude to Professor K.G. Bogolitsyn.

Funding

The work was performed within the framework of the state assignment of the Federal State Budgetary Educational Institution Federal Research Center for Comprehensive Study of the Arctic, Ural Branch of the Russian Academy of Sciences State Reg. No. 125021902595-1 for 2025–2027.

Conflict of interest

The authors declare that they have no conflict of interest.

References

- [1] A.N. Lachinov, N.V. Vorob'eva. *Phys. Usp.*, **49** (12), 1223 (2006). DOI: 10.3367/UFNr.0176.200612a.1249
- [2] E.I. Evstigneyev, D.N. Zakusilo, D.S. Ryabukhin, A.V. Vasilyev. *Russ. Chem. Rev.*, **92**(8), RCR5082 (2023). DOI: 10.59761/RCR5082.
- [3] M.B. Hocking. *J. Chem. Educ.*, **74** (9), 1055 (1997). DOI: 10.1021/ed074p1055
- [4] A. Llevot, E. Grau, S. Carlotti, S. Grelier, H. Cramail. *Macromol. Rapid Commun.*, **37**, 9 (2016). DOI: 10.1002/marc.201500474
- [5] L. Fakhra, X. Lingxia, I.K. Mahammed, A. Shehbaz, U.R. Mujeib, Z. Daochen. *Ind. Crops Prod.*, **204** (B), 117372 (2023). DOI: 10.1016/j.indcrop.2023.117372
- [6] L. Fang, Y. Tao, J. Zhou, C. Wang, M. Dai, J. Sun, Q. Fang. *Polym. Chem.*, **12** (5), 766 (2021). DOI: 10.1039/D0PY01653E
- [7] D. Menglu, T. Yangqing, F. Linxuan, W. Caiyun, S. Jing, F. Qiang. *ACS Sustainable Chem. Eng.*, **8** (39), 15013 (2020). DOI: 10.1021/acssuschemeng.0c05503
- [8] K.G. Bogolitsyn, S.S. Khviyuzov, M.A. Gusakova, M.A. Pustynnaya, A.A. Krasikova. *Wood Sci. Technol.*, **52** (4), 1153 (2018). DOI: 10.1007/s00226-018-1008-z
- [9] M.P. Tonkonogov. *Phys. Usp.*, **41**, 25 (1998). DOI: 10.1070/pu1998v041n01 abeh000328
- [10] A.K. Jonscher. *J. Phys. D*, **32**, 57 (1999). DOI: 10.1088/0022-3727/32/14/201
- [11] A. Chantal, T. Brotin, C. Garcia, F. Pelle, P. Goldner, B. Bigot, A. Collet. *J. Am. Chem. Soc.*, **116** (5), 2094 (1994). DOI: 10.1021/ja00084a055
- [12] S.K.K. Jatkar, C.M. Deshpande. *J. Ind. Chem. Soc.*, **37**, 1 (1960). DOI: 10.5281/zenodo.6531708
- [13] T. Blythe, D. Bloor. *Electrical Properties of Polymers* (Cambridge, CUP, 2005).
- [14] F. Kremer. *J. Non-Crystalline Solids*, **305** (1-3), 1 (2002). DOI: 10.1016/S0022-3093(02)01083-9

- [15] G.D. Kopusov, A.V. Tyagunin. *Fizika passivnykh dielektrikov* (SAFU, Arhangel'sk, 2013) (in Russian).
- [16] V.L. Bonch-Bruevich, S.G. Kalashnikov, *Fizika poluprovodnikov* (Nauka, M., 1977) (in Russian).
- [17] I.P. Zvyagin. *Kineticheskie yavleniya v neuporyadochennykh poluprovodnikakh*. (MGU, M., 1984). (in Russian).
- [18] S. Havriliak, S. Negami. J. Polym. Sci. C, **14**, 99 (1966). DOI: 10.1002/polc.5070140111
- [19] K.S. Cole, R.H. Cole. J. Chem. Phys., **9**, 341 (1941). DOI: 10.1063/1.1750906
- [20] D.W. Davidson, R.H. Cole. J. Chem. Phys., **19**, 1484 (1951). DOI: 10.1063/1.1748105
- [21] P. Debye. *Polar Molecules: Wisconsin Lectures* (Chemical, Catalog Co., N.Y., 1929).
- [22] A.S. Volkov, G.D. Kopusov, R.O. Perfil'ev, A.V. Tyagunin. Opt. Spectrosc., **124** (2), 202 (2018). DOI: 10.1134/S0030400X18020200
- [23] A.S. Volkov, G.D. Kopusov, R.O. Perfil'ev. Opt. Spectrosc., **125** (3), 379 (2018). DOI: 10.1134/S0030400X18090242
- [24] B.A. Belyaev, N.A. Drokin, V.F. Shabanov. Phys. Solid State, **48** (5), 973 (2006). DOI: 10.1134/S106378340605026X
- [25] S. Khviyuzov, K. Bogolitsyn, A. Volkov, G. Kopusov, M. Gusakova. Holzforschung, **74** (12), 1113 (2020). DOI: 10.1515/hf-2019-0149
- [26] K.G. Bogolitsyn, S.S. Khviyuzov. Pol. Bull., **80** (1), 1001 (2023). DOI: 10.1007/s00289-022-04323-x
- [27] K.G. Bogolitsyn, S.S. Khviyuzov, A.S. Volkov, G. D. Kopusov, M.A. Gusakova. Russ. J. Phys. Chem. A, **93**, 353 (2019). DOI: 10.1134/s0036024419020055
- [28] A.S. Volkov, G.D. Kopusov, S.S. Khviyuzov. Chem. Phys., **548**, 111202 (2021). DOI: 10.1016/j.chemphys.2021.111202
- [29] A.S. Volkov, S.S. Khviyuzov. J. Appl. Spectrosc., **90** (6), 1259 (2023). DOI: 10.1007/s10812-024-01662-7
- [30] S.S. Khviyuzov, A.S. Volkov. Polym. Adv. Technol., **35** (6), e6467 (2024). DOI: 10.1002/pat.6467

Translated by A. Akhtyamov